Available online at www.derpharmachemica.com

ISSN 0975-413X
CODEN (USA): PCHHAX

Der Pharma Chemica, 2016, 8(6):214-221
(http://derpharmachemica.com/archive.html)

Preparation and characterization of a vitreous phase and application as a corrosion inhibitor in acidic medium

A. Elbadaoui, M. Galai, M. Cherkaoui and T. Guedira

Laboratory of Materials, Electrochemistry and Environment, Faculty of Science, Ibn Tofail University, Kénitra, Morocco

---

ABSTRACT

The influence of (0.95-x) Bi2O3-x B2O3-0.05 (Ta2O5-Nb2O5) named A1 on the corrosion of steel in 1M HCl was investigated. Electrochemical polarization and impedance spectroscopic studies measurements were used. The inhibition efficiency increases with A1 content to reach 88% at 150 ppm. Polarisation curves show that A1 acts as a cathodic inhibitor. The increase in temperature leads to an decrease in the inhibition efficiency of the A1 inhibitor. The activation energies in the presence and absence of inhibitor have been determined and discussed.

Keywords: Steel; Corrosion; Inhibition; A1;polarization; impedance**.**

INTRODUCTION

The damage by corrosion generates not only high cost for inspection, repairing and replacement, but a public risk, thus, the need to implement protection systems such as corrosion inhibitors especially in acid media [1]. Acidic solutions are widely used in the industry such as the acid pickling of steel, the chemical cleaning, surface treatment ... The use of hydrochloric acid in pickling of metals and acidization of oil wells is more economical and efficient compared to other mineral acids [2]. Many inhibitors have been used in order to protect metals in acid environments [3-4]. However, the use of inorganic inhibitors such as polyphosphates, in particular metaphosphate glass, for corrosion inhibition has received considerable attention [5]. Polyphosphates are known to prevent the corrosion by inhibiting calcite crystallization [6].

In the present work, we have investigated the inhibitive action of a vitreous phase on corrosion of mild steel in HCl 1 mole/L using stationary polarization and electrochemical impedance. The effect of the temperature and the boron content in the glass layer was also studied. Thus, an action mechanism of the compound has been proposed.

MATERIALS AND METHODS

2.1. Electrochemical measurements

Before each experiment, the mild steel ((wt.%) C = 0.21, Mn = 0.05, Si = 0.38, S = 0.05, P = 0.09, Al = 0.01 and the remaining iron) was polished using emery paper until 1200 grade. After the substrate was degreased with ethanol, rinsed with distilled water and finally dried at room temperature. The aggressive solution (HCl 1 mole/L) was prepared by dilution of Analytical Grade 37% HCl with distilled water. Inhibitors corrosion was added at their powder form to corrosive solution in the range of 100–300 ppm concentrations (Table 1).

The electrolysis cell is a borrosilcate glass (Pyrex®) cylinder closed by cap with five apertures. Three of them were used for the electrodes. The reference electrode was a saturated calomel electrode (SCE). A platinum electrode was used as auxiliary electrode. The working electrode was carbon steel. The working electrode was immersed in the test solution for 30 min to establish a steady state open circuit potential (Eocp). The electrochemical measurements

were carried out using Potentiostat/Galvanostat/Voltalab PGZ 100 monitored by a personal computer using Tacussel corrosion analysis software model (Voltamaster 4).

The electrochemical behavior of sample in the inhibited and uninhibited solution was studied by recording anodic and cathodic potentiodynamic polarization curves. Measurements were performed in the 1M HCl solution containing different concentrations of the tested inhibitor by changing the electrode potential automatically from -900 mV to -100 mV versus corrosion potential at a scan rate of 1 mV s^{-1}. The linear Tafel segments of anodic and cathodic curves were extrapolated to corrosion potential to obtain corrosion current densities (Icorr).

Inhibiting efficiencies were calculated using the following equation:

$$\eta = \frac{i^0_{corr} - i_{corr}}{i^0_{corr}} \times 100 \quad (1)$$

Où i^0_{corr} et i_{corr} sont respectivement les valeurs de la densité de courant sans et avec inhibiteur. Where i^0_{corr} and i_{corr} s are respectively the values of the current density with and without inhibitor.

The EIS experiments were conducted in the frequency range with a high limit of 100 kHz and a different low limit 0.1 Hz at open circuit potential, with 10 points per decade, at the resting potential, after 30 min of acid immersion, by applying 10 mV ac voltage peak-to-peak. Nyquist plots were made from these experiments and the best semicircle can be fitted through the data points in the Nyquist plot using a non-linear least square fit so as to give the intersections with the x-axis.

The efficiency of inhibition was calculated from the relationship:

$$E_{R_{ct}}\% = \frac{R'_{ct} - R_{ct}}{R'_{ct}} \times 100$$

where R'_{ct} et R_{ct} are respectively the transfer of resistance values with and without the inhibitor.

All electrochemical tests have been performed in aerated solutions at 298 K

2.2 Synthesis of the vitreous phases of the system Bi_2O_3-B_2O_3-(Ta_2O_5-Nb_2O_5):

The vitreous phases of the system Bi_2O_3-B_2O_3-(Ta_2O_5-Nb_2O_5) are obtained by fusion of the stoechiometric mixtures of the starting products according to the reaction pathway:

(1-x-y)Bi_2O_3+xB_2O_3+y/2Ta_2O_5 + y/2Nb_2O_5 ⟶ x-y) Bi_2O_3+xB_2O_3+ y/2Ta_2O_5 + y/2Nb_2O_5.

The reagents closely are crushed in an agate mortar then introduced into alumina crucibles.

A first heat treatment was carried out with 350°C during one night followed by crushing; in continuation the temperature was increased by stage of 50 °C fine in order to avoid the chemical losses by volatilization ; followed by melting at 950 ° C.

The reactional mixture is then brought up to a higher temperature at the melting point. The molten mixture is then soaked with the free air in a mould out of alumina heated before hand with approximately 200°C.

The band between 1190-1240cm^{-1} is allotted to the vibration of the final groupings B-O^- in units pyroborates [7-9] .

On the other hand, the line around 1270-1310cm^{-1} is allotted to the asymmetrical mode of elongation B-O in the unit's orthoborate (BO_3).

The progressive adition of B2O3 causes an increase in the intensity of the bands located towards 420-490, 500-540,600-690 cm^{-1} andthe reduction in the intensity of the band around1190-1240cm^{-1} . The wide strip located around 980-1000 cm^{-1} is dominant.

Reduction in the intensity of line around 1190-1240 cm^{-1} assigned with the units pyroborates compared to that located towards 600 - 690 cm^{-1} relative with the métaborates are explained by the conversion of the units pyroborates into units métaborates.

However the reductionin the intensity of the band allotted to the pyroborates compared to the wide strip towards980-1000 cm^{-1} seems related to the conversion of the pyroborates into entities diborate. This transformation is probably related to the increase in the rate of boron atoms in co-ordination number IV.

The band between 640-650 cm^{-1} corresponds to the vibration of connection Ta-O and the band 870 cm^{-1} is allotted to the vibration of the connection Ta-O-Ta [11]

In general, in the beach from 600 to 950 cm^{-1} du Nb-O vibrations of elongation can be observed [12] The close band IR 920 cm^{-1} iallotted to the mode of stretching of connections Nb-O while strongest nearly 620 cm^{-1} was allotted to the stretching of more than bridging connections Nb-O-Nb deformed in NbO6 octahedral [13] . In particular in the area from 500 to 700 cm^{-1} area of vibrations of valence of Ta-O-Nb [14] .

2.3 Studies of glasses of compositions (0.95-x) Bi_2O_3-x B_2O_3-0.05 (Ta_2O_5-Nb_2O_5) :
Table 1 gives the molar fractions corresponds tothe compositions (0.95-x) Bi_2O_3-xB_2O_3-0.05(Ta_2O_5-Nb_2O_5).

Figure 1 represents the infra-red spectra of these compositions. The frequencies and their attributions are consigned in table 2.

Table 1 : Composition of the samples prepared within the system (0.95-x) Bi_2O_3-xB_2O_3-0.05 (Ta_2O_5-Nb_2O_5).

sample.N°	0.95-x	x
A_1	0.65	0.3
A_2	0.6	0.35
A_3	0.55	0.4
A_4	0.5	0.45
A_5	0.45	0.5

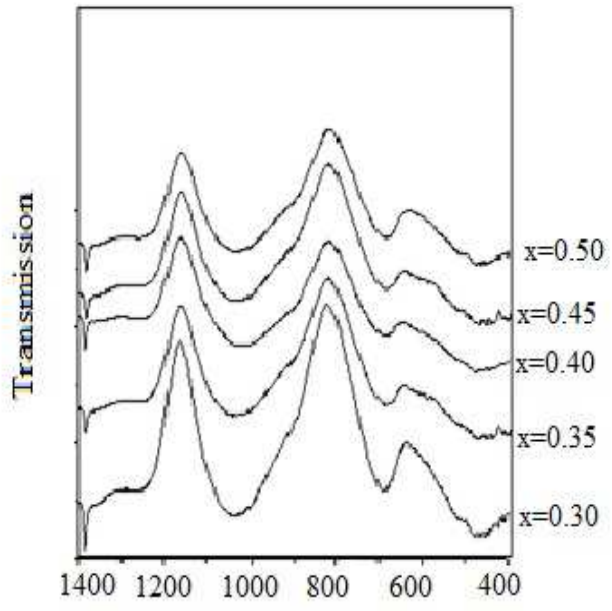

Figure 1: Spectra infra-red of glasses of compositions (0.95-x)Bi_2O_3-xB_2O_3-0.05 (Ta_2O_5- Nb_2O_5).

Table 2 : Attributions of the infra-red frequencies of glasses of compositions (0.95-x) Bi2O3-x B2O3-0.05(Ta2O5-Nb2O5).

N° the sample		A_1	A_2	A_3	A_4	A_5
Composition		x=0.30	x=0.35	x=0.4	x=0.45	x=0.5
Attributions	υ skeleton (Bi-O-Bi)	482	480	473	469	461
	υ skeleton (B-O-Bi)	----	426	427	438	449
	υ skeleton (B-O-B)	551	523	510	----	-----
	υ (Nb-O)	670	668	669	690	688
	υ (Nb-O-Nb)	637	636	620	625	----
	υ (Ta-O-Nb)	----	507	542	588	593
	υ (Ta-O)	----	----	----	----	----
	boroxol	----	----	----	----	----
	orthoborates BO_3	----	----	----	----	----
	υ_s BO (BO^{4-})	----	1002	1016	1034	1036
	Pyroborates B-O^-	1216	1243	1244	1249	1250
	υ_{as}(BO) dans BO_3	1316	----	----	----	----

The substitution of bismuth by boron involves an increase in the intensities of the bands B-O- Bi and a reduction in the intensities of the bands Bi--O-Bi.

We notice a disappearance of the band corresponding to the groupings orthoniobate υs (Nb-O-Nb).

We observe also a displacement of the bands assigned with the groupings méthaborates towards the low frequencies.

A disappearance of the inversion de υ_{as} (BO) in BO_3.

The increase in the content of Ta2O5 andNb2O5 in the system Bi_2O_3- B_2O_3- (Ta_2O_5-Nb_2O_5) involves:
- the disappearance of bands B-O-B.
- disappearance of the bands assigned with the groupings orthoborates .
- also found that there is a displacement of the band corresponds to pyroborates BO towards the high frequencies.

RESULTS AND DISCUSSION

3.1. Polarization curves

Figure 2 shows the effect of A_1 concentration on the cathodic and anodic polarization curves carried out on mild steel in HCl 1 mole/L. We observed a decrease of the cathodic and anodic currents with the addition of A1 which suggests that the anodic dissolution is reduced and the oxygen reduction is inhibited. The action on the cathodic area is greater. So we can classify this compound A_1 as mixed inhibitor acting on both areas, cathodic and anodic [15-17].

Electrochemical corrosion kinetics parameters, i.e. corrosion potential (E_{corr}) and corrosion current density (i_{corr}) obtained from the extrapolation of the polarization curves were given in Table 3. There was no definite trend is observed in the Ecorr values by against the corrosion current substantially decreases with the addition of compound A_1. A maximum of 88% efficiency is obtained for a concentration of 150 ppm. The corrosion inhibition property of A_1 can be attributed to its adsorption at the carbon steel surface.

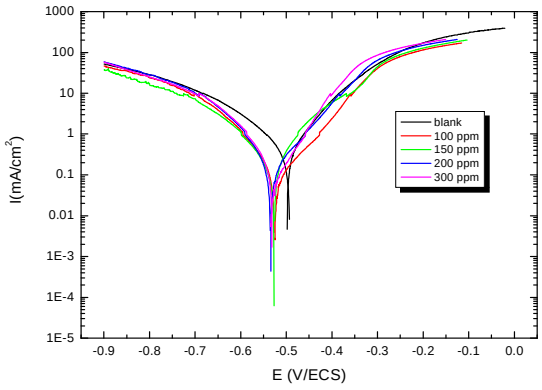

Figure 2. Typical polarization curves for corrosion of mild steel in 1 M HCl in the absence and presence of different concentrations of A_1

Table 3. Potentiodynamic polarization parameters without and with different concentrations of A_1 in 1 M HCl

C inh(M) de A1	Ecorr	I_{corr} (µA/cm²)	E%
Témoin	-497	983	-
100ppm	-525	152	84.5
150ppm	-526	115	88
200ppm	-533	177	82
300ppm	-530	201	79.5

3.2 Electrochemical impedance spectroscopy

Figure 3 shows the impedance spectra obtained in corrosion potential E_{corr} after 30 minutes of immersion. We see a capacitive loop assigned to the charge transfer of the corrosion process, the diameter increases with the concentration of A1 compound. To extract the electrochemical parameters, the model of the equivalent circuit used is shown in Figure 4. The highest resistance and therefore the most important efficiency are also achieved at a concentration of 150 ppm confirming the A1 inhibitor effect (table 4). The E (%) values obtained from the ac impedance technique are comparable and run parallel with those obtained from the potentiodynamic polarization method.

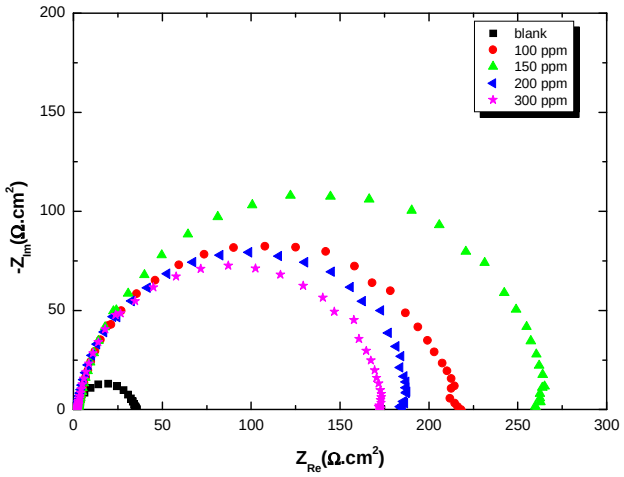

Figure 3: Nyquist diagrams for Carbon-steel electrode with and without A_1 at Ecorr after 30 min of immersion

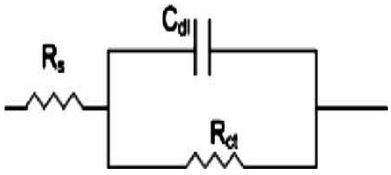

Figure 4 Equivalent circuit of the acid-metal interface

Table 4: Electrochemical impedance parameters in HCl 1 mol/L at different A1 concentration

Cinh (M) A1	R_{ct}(ohm.cm²)	C_{dl} (µf/cm²)	E%
témoin	35	284	-
100ppm	220	136	84
150ppm	268	111	87
200ppm	181	144	81
300ppm	175	152	80

3.3Effect of temperature

3.3.1 Potentiodynamic polarization measurements

Polarization curves for carbon steel electrode in the absence and the presence of A_1 with different temperatures (between 298 and 328 K) are showed in Figure 5. The related electrochemical parameters, i.e. corrosion potential (Ecorr) and corrosion current density (icorr) and the inhibition efficiency (Ect) values are listed in Table 5.

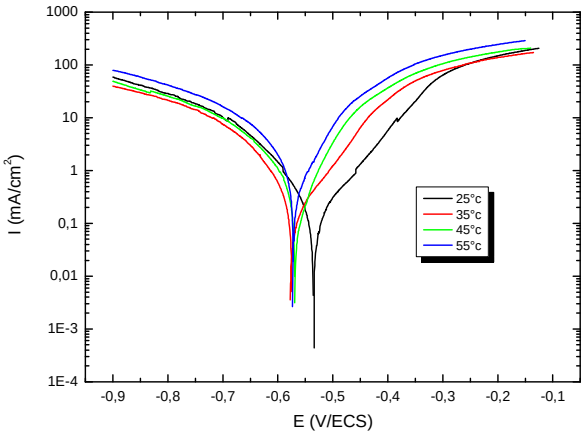

Figure 5: Potentiodynamic polarization curves for C-steel in 1 M HCl + 150 ppm of A_1 at different temperatures

Table 5: Electrochemical impedance parameters in HCl 1 mol/L at different A1 temperatures

	Ecorr(mV/Ag/Agcl)	Icorr(mA/cm²)
25C°	-498	0.983
35 C°	-491	1.6
45 C°	-475	2.42
55 C°	-465	3.1

We note that Ecorr values become slightly more negative and Icorr values increase with the temperature indicating a deterioration of the substrate.

To investigate the mechanism of inhibition, the activation parameters for the corrosion process were calculated from Arrhenius type plot according to the following equation [18-20] .

$$Ln\left(\frac{1}{R_{ct}}\right) = -\frac{E_a}{RT} + LnA$$

Where Ea : The apparent activation energy, A : The pre-exponential factor, R : The universal gas constant and T : The absolute temperature.

Moreover, the Arrhenius equation can be converted an alternative equation as follow [21] :

$$\frac{1}{R_{ct}} = \frac{RT}{Nh}\exp\left(\frac{\Delta S_a^*}{R}\right)\exp\left(\frac{\Delta H_a^*}{RT}\right)$$

Where h is Planck's constant, N Avogadro's number, R the universal gas constant, ΔH^*_a the enthalpy of the activation and ΔS^*_a is the entropy of activation.

Variations of Ln (I corr = $1/R_{ct}$) as a function of inverse temperature are shown in Figure 6. We observe a linear variation with correlation coefficients (C.C) near 1 with a slope of $\Delta H^*_a/R$.

The Table 6 shows that values of E_a and ΔH_a obtained in presence of A_1 are higher than those obtained in the inhibitor-free solution. This result confirms the adsorption of the inhibitor on the surface of the steel.

Table 6: The value of activation parameters Ea, ΔH^*_a and ΔS^*_a for Carbon-steel in HCl M in the absence and presence of 150 ppm of A1.

	E_a KJ/mol	ΔH^*_a KJ/mol	ΔS^*_a KJ/mol
Without inhibitor	31.5	28	-107
With 150 ppm A1	47.1	44.5	17.23

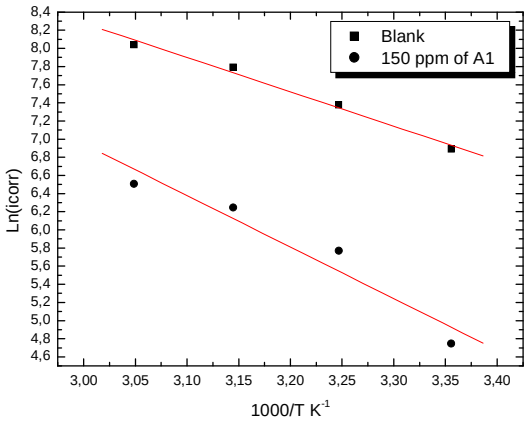

Figure 6: Arrhenius plots of Carbon -steel in 1 M HCl with and without 150ppm of A_1

3.4 Effect of Borate content in glass

The corrosion behavior of mild steel in 1 M HCl solution for different compositions of glasses in the system (0.95-x) Bi_2O_3-x B_2O_3-0.05 at 150 ppm, was investigated using EIS at room temperature after 30 mn of immersion at corrosion potential. Figure 7 shows the impedance (Nyquist) spectra. To extract the electrochemical parameters, the model of the equivalent circuit used is shown in Figure 4. The electrochemical parameters derived from the Nyquist plots and inhibition efficiencies values are given in Table 6. We note that the resistance transfer and therefore the steel strength increase with borate content. Indeed, borates promote the absorption of oxygen and inhibit its reduction.

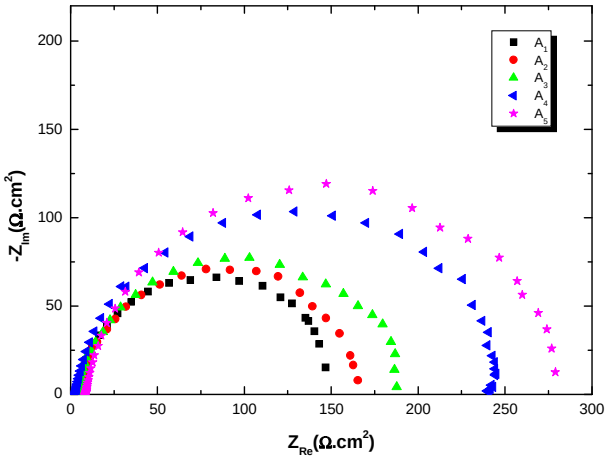

Fig. 7: Impedance diagram of mild steel recoded in 1 M HCl containing 150 ppm of each (0.95-x) Bi_2O_3-x B_2O_3-0.05(Ta_2O_5-Nb_2O_5) at corrosion potential (x varied from 0.3% to 0.5%).

Table.6:Electrochemical parameters derived from the Nyquist plots and inhibition efficiencies values for mild steel in 1 M HCl containing 150ppm of (0.95-x) Bi_2O_3-x B_2O_3-0.05(Ta_2O_5-Nb_2O_5) glass system (x varied from 0.3% to 0.5%).

Cinh (M)	Rct(ohm.cm²)	Cdl(µf/cm²)
A1	149	194
A2	165	181
A3	191	131
A4	268	111
A5	280	99

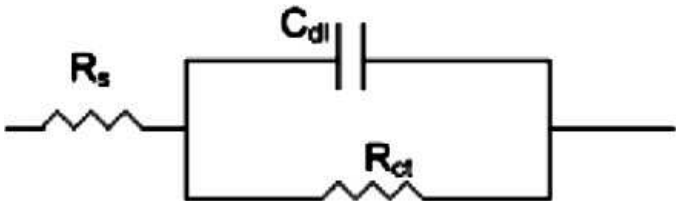

Fig. 8: Equivalent circuit for the metal–acid interface

CONCLUSION

The corrosion inhibition of mild steel in acidic medium by the phosphate glasses was studied by polarization curves and electrochemical impedance spectroscopy. The obtained result show that all glasses make a good inhibition. This inhibition depends on the bore in the glasses system and decrease with decreasing B_2O_3 content and make by the formation of protective film based B_2O_3.

The inhibition efficiency of A1 is temperature-dependent, and inhibition efficiency decreases slightly with the increase in the temperature. The addition of A1 leads to a increase in activation corrosion energy.

REFERENCES

[1]G. Trabanelli, *Corrosion* (**1991**), 47, 410.
[2] D.D.N. Singh, T.B. Singh, B. Gaur, *Corros. Sci*. (**1995**) 37,1005.
[3] Xiang-Hong Li, Shu-Duan Deng, Fu Hui, *J. Appl. Electrochem*. (**2010**) 40 , 1641– 1649
[4] E. Lazarova, G. Petkova, T. Iankova, L. Ivan, G. Neikov, *J. Appl. Electrochem*. (**2008**) 28, 1391–1399.
[5] O. Lahodny-Sˆarc, L. Kaštelan, *Corros. Sci*. (**1976**) 16, 25–34.
[6] O. Lahodny-Sˆarc, L. Kaštelan, *Corros. Sci*. (**1976**) 16,25–34.
[7]-E.I.Kamitos, G.A.Karakasside and G.D.Chryssikos, *Phys,Chem;Glasses* (**1987**) 28.
[8] M.Villa, G Chiodelli,M.Scagliotti,*Solid State ionics* , (**1986**) 18-19, 382-387.
[9] J.F.Ducel,These de Doctorat, Université Bordeaux I,N°955(**1993**).
[10] J. Masse, H. Szymanowski, O. Zabeida, A. Amassian, J.E. Klemberg- Sapieha, L. Martinu, Stability and effect of annealing on the optical properties of plasma-deposited Ta_2O_5 and Nb_2O_5 films, *Thin Solid Films* (**2006**) 515,1674–1682.
[11]B.B.Meera,A.K.Sppd,N.chandradhas and J.Ramakrishna. *Journal of Non-Crystalline Solids* (**1990**) 126, 224.
[12] A. Pawlicka, M. Atik, MA Aegerter *Thin Solid Films*, (**1997**), 301,p. 236
[13] T. Armaroli, G. Busca, C. Carlini, M. Giuttari, AMR Galletti, G. Sbrana *J. Mol. Catal*. A, (**2000**), 151,p. 233.
[14] MG Zuev, AA Fotiev, IE Lobov *Russ. J. Inorg. Chem*. (Engl. Transl.), (**1990**) 35, pp. 152154.
[15] A.K. Singh, M. A. Quraishi, *Corros. Sci*. (**2010**) 52, 1529
[16] O. L. Riggs Jr., Corrosion Inhibitors, 2nd ed., (**1973**) C.C. Nathan, Houston, TX .
[17] K. F. Khaled, N. Hackerman, *Electrochim. Acta* (**2003**) 48, 2715
[18]-EE Oguzi; CB Adindu; CK Enenebeak; CE Ogukwe; MA Chidiebere; KL Oguzie, *J Phys Chem*., **2012**,C116 ,13603
[19] X Li; S Deng; H Fu,*Corros Sci*., **2011**, 53, 664
[20] X Li; S Deng; H Fu, *Corros Sci*., **2012**, 55, 280
[21] [E. A. Noor, A. H. Al-Moubaraki, *Mater. Chem. Phys*. (**2008**) 110, 145]